JOURNAL OF GUIDANCE, CONTROL, AND DYNAMICS
Vol. 28, No. 4, July–August 2005

Engineering Notes

ENGINEERING NOTES are short manuscripts describing new developments or important results of a preliminary nature. These Notes should not exceed 2500 words (where a figure or table counts as 200 words). Following informal review by the Editors, they may be published within a few months of the date of receipt. Style requirements are the same as for regular contributions (see inside back cover).

Continuous Traditional and High-Order Sliding Modes for Satellite Formation Control

Timothy Massey*
Science Applications International Corporation, Huntsville, Alabama 35806
and
Yuri Shtessel†
University of Alabama in Huntsville, Huntsville, Alabama 35899

I. Introduction

THIS Note focuses on continuous traditional and high-order sliding mode control for controlling the motion of one satellite as it follows a defined path around another satellite that is orbiting the Earth robustly to model uncertainties and external disturbances. The problem with any satellite formation control is that all orbiting bodies are subject to forces that tend to force the satellites out of their stable Keplerian orbits.[1] These forces include gravitational perturbations, atmospheric drag, and solar radiation pressure.[2] Recently Yeh et al.[3] defined an effective robust method of controlling satellites using sliding mode control (SMC)[4] while minimizing fuel consumption.

Because the satellites are usually controlled by the thrusters, a relay SMC with a dead band is used.[3] The width of the dead band, δ, is selected[3] to minimize the fuel consumption. At the same time, simulations show that the jet-thruster duty cycle depends on a board computer step size. This means that using a dead-band controller does not allow control of the frequency of switching. This could create a problem in using SMC in satellite formation control actuated by jet thrusters that can be switched on and off with a required duty cycle.

To address the problem, one may use high-gain continuous approximation of the relay function with consecutive pulse-width modulation (PWM) of continuous control to stabilize the duty cycle of the thruster. However, this introduces two sets of accuracy losses to the system, one from the continuous approximation and one from the PWM technique. This Note proposes a way to eliminate one of these losses by using recently developed continuous SMC techniques, including high-order sliding mode (HOSM) control algorithms,[5] SMC driven by a sliding mode observer,[4] and asymptotic HOSM using an integral sliding variable[6] that outputs continuous control signals without high gain continuous approximations of discontinuous SMC followed by a PWM to control the duty cycle. The main contribution of this Note is further improving SMC for satellite formation control[1–3] via application of recently developed continuous SMC algorithms modulated by PWM, allowing high tracking accuracy in the presence of bounded matched disturbances and uncertainties and providing a required duty cycle in a control command to the jet thrusters.[7] The studied continuous SMCs provide low weekly fuel consumption.

II. Continuous Sliding Mode Control

In this section the continuous SMC techniques that combined with PWM are applied to controlling a multiple satellite formation are considered.

Consider a nonlinear multi-input/multi-output system

$$\dot{\boldsymbol{x}} = f(\boldsymbol{x}, t) + G(\boldsymbol{x}, t)\boldsymbol{u}, \qquad \boldsymbol{y} = h(\boldsymbol{x}, t) \tag{1}$$

where $\boldsymbol{x} \in \Re^n$, $\boldsymbol{y} \in \Re^m$, $\boldsymbol{u} \in \Re^m$ and $f(\boldsymbol{x}, t) \in \Re^n$, $h(\boldsymbol{x}, t) = [h_1, h_2, \ldots, h_m]^T \in \Re^m$, $G(\boldsymbol{x}, t) = [g_1, g_2, \ldots, g_m] \in \Re^{n \times m}$, $g_i \in \Re^n \; \forall \, i = \overline{1, m}$ are analytic vector and matrix functions. Assuming the system (1) is completely feedback linearizable[8] in a reasonable domain $\boldsymbol{x} \in \Gamma$, the system is transformed to a regular format:

$$\begin{bmatrix} \boldsymbol{y}_1^{(r_1)} \\ \boldsymbol{y}_2^{(r_2)} \\ \cdots \\ \boldsymbol{y}_m^{(r_m)} \end{bmatrix} = \begin{bmatrix} L_f^{r_1} h_1(x, t) \\ L_f^{r_2} h_2(x, t) \\ \cdots \\ L_f^{r_m} h_m(x, t) \end{bmatrix} + E(\boldsymbol{x}, t)\boldsymbol{u} \tag{2}$$

$$E(\boldsymbol{x}, t) = \begin{bmatrix} L_{g_1}\left(L_f^{r_1 - 1} h_1\right) & L_{g_2}\left(L_f^{r_1 - 1} h_1\right) & \ldots & L_{g_m}\left(L_f^{r_1 - 1} h_1\right) \\ L_{g_1}\left(L_f^{r_2 - 1} h_2\right) & L_{g_2}\left(L_f^{r_2 - 1} h_2\right) & \ldots & L_{g_m}\left(L_f^{r_2 - 1} h_2\right) \\ \cdots & \cdots & \cdots & \cdots \\ L_{g_1}\left(L_f^{r_m - 1} h_m\right) & L_{g_2}\left(L_f^{r_m - 1} h_m\right) & \ldots & L_{g_m}\left(L_f^{r_m - 1} h_m\right) \end{bmatrix} \tag{3}$$

where $|E(\boldsymbol{x}, t)| \neq 0 \; \forall \, \boldsymbol{x} \in \Gamma$, $L_f^{r_i} h_i$ and $L_{g_i}(L_f^{r_i - 1} h_i) \; \forall \, i = \overline{1, m}$ are corresponding Lie derivatives (see Ref. 8), and $\bar{\boldsymbol{r}} = [r_1, r_2, \ldots, r_m]^T$ is a vector relative degree. Introducing a desired decoupled output tracking compensated dynamics as

$$\sigma_i = e_i^{(r_i - 1)} + c_{i, r_i - 2} e_i^{(r_i - 2)} + \cdots + c_{i,1} e_i^{(1)} + c_{i,0} e_i + c_{i,-1} e_{i,-1} = 0 \qquad \forall i = \overline{1, m} \tag{4}$$

where $e_i = y_{i,c}(t) - y_i(t)$, $y_{i,c}(t)$ is the ith output command profile,

$$e_i^{(j)} = \frac{\mathrm{d}^j e_i}{\mathrm{d}t^j}, \qquad e_{i,-1} = \int e_i \, \mathrm{d}t$$

and the coefficients $c_{i,j} \; \forall \, i = \overline{1, m} \; \forall \, j = \overline{-1, r_i - 2}$ are chosen to achieve the desired eigenvalue placement in the decoupled differential–integral equations (4). In terms of SMC, $\boldsymbol{\sigma} = [\sigma_1, \sigma_2, \ldots, \sigma_m]^T \in \Re^m$ is called a vector sliding variable, and in Eq. (4), $\boldsymbol{\sigma} = 0$, is called a sliding surface.

The problem is to design SMC $\boldsymbol{u}$ to provide decoupled asymptotic output tracking: $e_i(t) \to 0$ as time increases by providing stability to the sliding variable dynamics, which is derived as

$$\dot{\boldsymbol{\sigma}} = \Psi(.) - E(\boldsymbol{x}, t)\boldsymbol{u} \tag{5}$$

Presented as Paper 2004-5021 at the AIAA Guidance, Navigation, and Control Conference, Providence, RI, 16–19 August 2004; received 20 October 2004; revision received 13 February 2005; accepted for publication 21 February 2005.

*System Engineer, 6725 Odyssey Drive.
†Professor, Electrical and Computer Engineering, 301 Sparkman Drive. Associate Fellow AIAA.

where $\psi_i(.) = y_{i,c}^{(r_i)} + c_{i,r_i-2}e_i^{(r_i-1)} + \cdots + c_{i,1}e_i^{(2)} + c_{i,0}e_i^{(1)} + c_{i,-1}e_i - L_f^{r_i}h_i(x,t)\,\forall\, i = \overline{1,m}$ and $\Psi(.) = [\psi_1(.), \ldots, \psi_m(.)]^T \in \Re^m$.

To separate the control design into m single-input/single-output control designs, a new control variable is introduced as

$$\tilde{\boldsymbol{u}} = E(\boldsymbol{x})\boldsymbol{u} \tag{6}$$

This allows Eq. (5) to be rewritten in a scalar format as

$$\dot{\boldsymbol{\sigma}}_i = \psi_i^0(.) + \Delta\psi_i(.) - \tilde{u}_i \tag{7}$$

where $\boldsymbol{v} = [v_1, \ldots, v_m]^T$, $\boldsymbol{\Psi}(.) = \boldsymbol{\Psi}^0(.) + \boldsymbol{\Delta\Psi}(.)$ with $\boldsymbol{\Psi}^0(.) = [\psi_1^0(.), \ldots, \psi_m^0(.)]^T \in \Re^m$, and $\boldsymbol{\Delta\Psi}(.) = [\Delta\psi_1(.), \ldots, \Delta\psi_m(.)]^T \in \Re^m$ are a known and unknown (due to external disturbances and model uncertainties) vectors, respectively. The unknown vector is assumed bounded: $\|\Delta\psi_i(.)\| \le L_i\,\forall\, i = \overline{1,m}\,\forall\, x \in \Gamma$.

A. Continuous SMC Driven by Sliding Mode Disturbance Observer

To design the sliding mode disturbance observer (SMDO) for estimating the bounded disturbance $\Delta\psi_i(.)$, the auxiliary sliding variables are introduced:

$$s_i = \sigma_i + z_i, \qquad \dot{z}_i = -\psi_i^0 + \tilde{u}_i - v_i \tag{8}$$

The s_i dynamics are derived taking into account Eqs. (7) and (8),

$$\dot{s}_i = \Delta\psi_i - v_i \tag{9}$$

It is easy to show[4,7] that the auxiliary sliding variables s_i are stabilized at zero by means of auxiliary SMC v_i:

$$v_i = (L_i + \rho_i)\,\mathrm{sign}(s_i), \qquad \rho_i > 0 \tag{10}$$

in a finite time $t_{ri} \le |s_i(0)|/\rho_i$. Therefore, equivalent control $v_{i\,\mathrm{eq}}$ exactly estimates the disturbance $\Delta\psi_i(.)\,\forall\, t \ge t_{ri}$, that is, $v_{i\,\mathrm{eq}} = \Delta\psi_i(.)$ in SMDO (8–10). To compute $v_{i\,\mathrm{eq}}$, high-frequency switching control (10) is processed by a low-pass filter[9] (LPF):

$$\hat{v}_{i\,\mathrm{eq}} = \mathrm{LPF}(v_i) \tag{11}$$

where $\hat{v}_{i\,\mathrm{eq}}$ can estimate $v_{i\,\mathrm{eq}}$ and, consequently, the disturbance $\Delta\psi_i(.)$ only asymptotically or, in a case of nonpiecewise constant disturbances, with a small error that is proportional to the time constant of LPF. For instance, if LPF is implemented as a simplest first-order lag block,

$$\hat{v}_{i\,\mathrm{eq}}(s) = [1/(\beta s + 1)]v_i(s) \tag{12}$$

where s is a Laplace variable, then $\lim \|v_{i\,\mathrm{eq}} - \hat{v}_{i\,\mathrm{eq}}\| \sim \beta$ and, consequently, $\lim \|\Delta\psi_i - \hat{v}_{i\,\mathrm{eq}}\| \sim \beta$ as $t \to \infty$. Note that the time constant of the filter can be taken to be very small, having a duty cycle of control (10) as a lower boundary.[4]

Consequently, an SMDO that estimates the disturbance $\Delta\psi_i$ is estimated by Eqs. (7–12) as $\Delta\hat{\psi}_i = \hat{v}_{\mathrm{eq}1}$. To achieve better attenuation in filtering Eqs. (11) and (12), the amplitude of v_i can be reduced in the sliding mode $s_i = 0$ using gain adaptation[4,7]:

$$v_i = \begin{cases} (L_i + \rho_i)\,\mathrm{sign}(s_i), & \text{if} \quad |s_i| > \mu_i \\ (|\hat{v}_{i\,\mathrm{eq}}| + \rho_i)\,\mathrm{sign}(s_i), & \text{if} \quad |s_i| \le \mu_i \end{cases} \tag{13}$$

where $\mu_i \sim$ to a computer step size T. The SMDO (7–13) is called an adaptive gain SMDO.

The SMC-based control $\tilde{\boldsymbol{u}}_i$ driven by SMDO (7–13) that asymptotically stabilizes the sliding variable $\boldsymbol{\sigma}_i$ at zero in presence of unknown bounded disturbance $\Delta\psi_i(.)$ is designed as follows:

$$\tilde{\boldsymbol{u}}_i = \psi_i^0(.) + K_{0i}\sigma_i + \hat{v}_{i\,\mathrm{eq}} \tag{14}$$

Indeed, substituting Eq. (14) into Eq. (7), we obtain

$$\dot{\sigma}_i = -K_{0i}\sigma_i - \hat{v}_{i\,\mathrm{eq}} + \Delta\psi_i(.) \tag{15}$$

As time increases, Eq. (15) tends to

$$\dot{\sigma}_i = -K_{0i}\sigma_i, \qquad K_{0i} > 0 \tag{16}$$

Finally, SMC $\boldsymbol{u}$ in Eq. (1) driven by SMDO (7–13) asymptotically stabilizes the vector sliding variable $\boldsymbol{\sigma}$ in Eq. (5) at zero is of the form $\boldsymbol{u} = E^{-1}(\boldsymbol{x})\tilde{\boldsymbol{u}}$.

B. Super-Twisting High (Second)-Order SMC

The intrinsic difficulties of the traditional SMC,[4] including chattering and applicability to systems with relative degree 1, are mitigated by the HOSM that stabilizes at zero not only the sliding variable, but also its $k-1$ successive derivatives (kth-order HOSM).[5] The approach is effective for arbitrary relative degrees, and the well-known chattering effect is significantly reduced because the high-frequency switching is hidden in the higher derivative of the sliding variable. When implemented in discrete time, HOSM provides for sliding accuracy proportional to kth power of the time increment, which makes HOSM an enhanced-accuracy robust control technique. The second-order SMC (SOSM),[5] in particular a super-twisting algorithm, is used to robustly stabilize $\boldsymbol{\sigma}_i$ in Eq. (7) at zero in a finite time in the presence of a bounded disturbance $\Delta\psi_i(.)$.

The super-twisting SOSM control[5] is based on the analysis of the perturbed nonlinear differential equation

$$\dot{q} + \alpha|q|^{\frac{1}{2}}\,\mathrm{sign}(q) + \beta\int \mathrm{sign}(q)\,\mathrm{d}\tau = \xi(t), \qquad |\dot{\xi}(t)| \le C \tag{17}$$

It is well known[5] that a solution $q(t)$ of Eq. (17) and its derivative $\dot{q}(t)$ converge to zero in a finite time if $\alpha \ge 0.5\sqrt{C}$ and $\beta \ge 4C$.

When the super-twist control

$$\tilde{u}_i = \psi_i^0(.) + \alpha_i|\boldsymbol{\sigma}_i|^{\frac{1}{2}}\,\mathrm{sign}(\boldsymbol{\sigma}_i) + \beta_i\int \mathrm{sign}(\boldsymbol{\sigma}_i)\,\mathrm{d}t \tag{18}$$

is substituted into Eq. (7), the $\boldsymbol{\sigma}_i$ compensated dynamics are achieved:

$$\dot{\boldsymbol{\sigma}}_i + \alpha_i|\boldsymbol{\sigma}_i|^{\frac{1}{2}}\,\mathrm{sign}(\boldsymbol{\sigma}_i) + \beta_i\int \mathrm{sign}(\boldsymbol{\sigma}_i)\,\mathrm{d}\tau = \Delta\psi_i(.) \tag{19}$$

Comparing Eqs. (17) and (19), one can conclude that selecting parameters of the super-twist controller (18) satisfies the inequalities $\alpha_i \ge 0.5\sqrt{L_i}$ and $\beta_i \ge 4L_i$, the sliding variable, and its derivative $\boldsymbol{\sigma}_i, \dot{\boldsymbol{\sigma}}_i \to 0$ in a finite time via control (18). Note that the control function $\tilde{u}_i$ in Eq. (18) is continuous because the discontinuous high-frequency portions, $\mathrm{sign}(\boldsymbol{\sigma}_i)\,\forall\, i = \overline{1,3}$, are integrated. Finally, vector super-twisting SOSM control $\boldsymbol{u}$ in Eq. (1) given in the form $\boldsymbol{u} = E^{-1}(\boldsymbol{x})\tilde{\boldsymbol{u}}$, with $\tilde{\boldsymbol{u}}_i$ defined by Eq. (18), stabilizes the vector-sliding variable $\boldsymbol{\sigma}$ in Eq. (5) at zero in a finite time. The output tracking errors e_i are stabilized at zero asymptotically due to Eq. (4) in the sliding mode $\boldsymbol{\sigma} = 0$ in the presence of bounded disturbances.

C. Continuous SMC by Using Integral Sliding Surfaces

A method of creating a Lyapunov-based, continuous SMC that is robust to matched disturbances is developed using an integral sliding surface (ISS).[6] SMC/ISS-based continuous control $\tilde{\boldsymbol{u}}_i$ that robustly asymptotically stabilizes $\boldsymbol{\sigma}_i$ in Eq. (7) at zero uses two sliding variables: $\boldsymbol{\sigma}_i$ and auxiliary integral sliding variable η_i:

$$\eta_i = \boldsymbol{\sigma}_i + \tilde{k}_{0i}s_i, \qquad \dot{s}_i = \mathrm{sign}(\boldsymbol{\sigma}_i) \tag{20}$$

and is designed in the form

$$\tilde{u}_i = \psi_i^0(.) + \left(\tilde{\rho}_i \big/ 2^{a_i}\right)|\eta_i|^{2a_i - 1}\,\mathrm{sign}(\eta_i), \qquad 0.5 < a_i < 1.0 \tag{21}$$

The following theorem was formulated and proven.

Theorem: Let $\tilde{\rho}_i > 0, \tilde{k}_{0i} > 0, a_i \to 1, |\Delta\ddot{\psi}_i(.)| \le \tilde{L}_i$, and $\dot{\sigma}_i^2/|\sigma_i| \le M < \infty$ in a bounded domain $D_i : \{\sigma_i, \dot{\sigma}_i\}$ containing the origin: then the continuous control (21), provides for the local asymptotic convergence of the sliding variable $\boldsymbol{\sigma}_i$ into a second-order sliding mode: $\dot{\boldsymbol{\sigma}}_i = \boldsymbol{\sigma}_i = 0$. Proof is given in the Appendix.

Finally, continuous SMC/ISS control $\boldsymbol{u}$ in Eq. (1) given in the form $\boldsymbol{u} = E^{-1}(\boldsymbol{x})\tilde{\boldsymbol{u}}$ with $\tilde{u}_i$ defined by Eq. (21) locally asymptotically stabilizes the vector sliding variable $\boldsymbol{\sigma}$ in Eq. (5) at zero. The output tracking errors e_i are stabilized at zero asymptotically due to Eq. (4) in the sliding mode $\sigma = 0$ in presence of bounded disturbances.

D. Discussion

The common feature of the SMC given in Secs. II.A, II.B, and II.C is that all of them are not continuous approximations of an ideal discontinuous SMC and they stabilize the sliding variables $\boldsymbol{\sigma}_i \; \forall \, i = \overline{1, 3}$ at zero in presence of external bounded disturbances. To control the satellite formation by using jet thrusters, the outputs of the proposed continuous SMC are transformed to a pulse train with a given duty cycle using PWM.

III. Leader/Follower Satellite Formation Mathematical Model

The formation control problem being studied in this Note is a two-satellite formation. The coordinate system used is shown in Fig. 1. The first satellite, the leader, is in a circular orbit around a spherical Earth, and, for simplicity, is assumed to maintain that orbit in free flight. Assuming the second satellite is in a slightly elliptical orbit but remains close to the first when compared to the overall radii of their orbits around the Earth, we use the linearized Hill equations to describe the relative motion between a leader and follower satellite. Because thrust levels are very low in many satellite applications, initial misalignments, as well as transients resulting from disturbances, may take many hours and even days to settle out. Thus, when the natural time t is scaled, a new time τ is defined such that $\omega t = \tau$, where ω is the mean motion of the leader around the Earth (a value of a constant angular velocity that is required for a satellite to complete one revolution). The normalized Hill equations in the new time τ are

$$\ddot{x} - 2\dot{y} - 3x = u_x + d_x, \qquad \ddot{y} + 2\dot{x} = u_y + d_y$$
$$\ddot{z} + z = u_z + d_z \tag{22}$$

In Eq. (22), u_x, u_y, and u_z are the net (difference between leader and follower) specific control forces acting on the follower satellite and d_x, d_y, and d_z encompasses the net specific disturbances experienced by the two-satellite system, including linearization residuals. The specific control forces and disturbances are the forces per unit mass per mean motion squared, ω^2. All terms in Eq. (22) have a length dimension. The coordinates x, y, and z describe the position of the follower satellite relative to the leader satellite. Parameterizing Eq. (22) as a function of τ with all external forces (control and disturbances) equal to zero provides the reference trajectories for the simulation[1,2]:

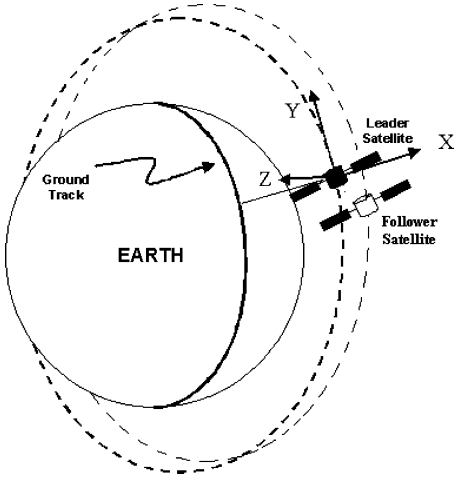

Fig. 1 Satellite formation coordinate system.

$$x_c(\tau) = r\sin(\tau + \theta), \qquad y_c(\tau) = 2r\cos(\tau + \theta)$$
$$z_c(\tau) = mr\sin(\tau + \theta) + 2nr\cos(\tau + \theta) \tag{23}$$

where r, m, n, and θ are arbitrary constants that define the elliptical desired path that the follower satellite maintains relative to the leader in a force free environment. In particular, r gives the size of the ellipse, θ is the initial angular position of the follower satellite on the path, and m and n are the slopes of the plane in which the path is located.

For any given θ, the follower satellite must enter the path (23) at initial conditions that are derived by setting $\tau = 0$ in Eq. (23), as well as in the derivative of Eq. (23), yielding

$$x_c(0) = r\sin(\theta), \qquad y_c(0) = 2r\cos(\theta)$$
$$z_c(0) = mr\sin(\theta) + 2nr\cos(\theta)$$
$$\dot{x}_c(0) = r\cos(\theta), \qquad \dot{y}_c(0) = -2r\sin(\theta)$$
$$\dot{z}_c(0) = mr\cos(\theta) - 2nr\sin(\theta) \tag{24}$$

The value of θ simply defines the angle at which the follower satellite is making with a reference coordinate of the leader. Physically, Eqs. (23) provide a circular or elliptical (depending on the choice of constants) reference trajectory around a leader satellite starting with the initial conditions defined in Eqs. (24).

IV. Satellite Formation Control in Continuous Sliding Modes

If there is a mismatch between the follower satellite and the reference trajectory, then the starting point for the satellite will not be on one of the desired trajectories and a control system will be required to get the follower satellite back on track. The disturbances d_x, d_y, and d_z, which are due to the oblateness of the Earth, atmospheric drag, tesseral resonance, solar radiation pressure (so-called J_2 effects) and bulges of the Earth (so-called J_3 effects) will gradually disperse an uncontrolled formation. The J_2 effect is by far the dominant perturbation force, followed by J_3. For this study, the representative d_x, d_y, and d_z disturbances are sine waves with up to 50% amplitude of a control thrust and a frequency of 0.6 rad/s (τ) and are kept the same for all of the controllers studied. Because SMC is insensitive to the matched disturbances, they will affect the fuel consumption only, retaining the same transient response in the sliding mode. Also we assume that the leader satellite is maintained on the orbit by its own control.

The problem is to improve the performance of discontinuous SMC with the dead band,[3] which cannot maintain a given duty cycle for jet thrusters, by designing the net control forces u_x, u_y, and u_z that robustly drive the follower satellite to the reference trajectory (23). This is accomplished by using continuous SMC/HOSM techniques studied in Sec. II, which are implemented using PWM to preserve a required frequency of thrusters' switching (duty cycle). The continuous SMC/HOSM controllers completely compensate for the bounded disturbances d_x, d_y, and d_z.

Considering relative positions x, y, and z in Eq. (22) to be measured, the vector-relative degree for the system (22) is identified as $\bar{\boldsymbol{r}} = (2, 2, 2)^T$ and the sliding variables (4) are formed:

$$\boldsymbol{\sigma} = [\sigma_x, \sigma_y, \sigma_z]^T, \qquad \boldsymbol{\sigma}_i = \dot{e}_i + c_{i,0}e + c_{i,-1}\int e_i \, \mathrm{d}\tau \qquad \forall i = x, y, z$$
$$e_x = \boldsymbol{x}_c - \boldsymbol{x}, \qquad e_y = \boldsymbol{y}_c - \boldsymbol{y}, \qquad e_z = z_c - z \tag{25}$$

The integral terms in Eq. (25) are added[4] to compensate for constant perturbations that could occur in sliding modes on the implementation step. The following optimized for fuel consumption compensated dynamics of the output tracking errors in the sliding mode in a normalized time τ are derived[3]:

$$\sigma_i(\tau) = \dot{e}_i + 1.8e_i + 1.0\int e_i \, \mathrm{d}\tau = 0 \rightarrow \ddot{e}_i + 1.8\dot{e}_i + 1.0e_i = 0 \qquad \forall i = x, y, z \tag{26}$$

A. Satellite Formation Control via Continuous SMC Driven by SMDO

The SMC-based controller driven by SMDO (8–14) is designed [where $u_i = \tilde{\boldsymbol{u}}_i$ because $E(\boldsymbol{x}) = I$ in Eq. (22)] for controlling the satellite formation model (22) and (23):

$$u_i = 10\sigma_i + \hat{v}_{i\,\mathrm{eq}}, \qquad \forall i = x, y, z$$

$$\dot{\hat{v}}_{i\,\mathrm{eq}} = 20[-\hat{v}_{i\,\mathrm{eq}} + 2\,\mathrm{sign}(s_i)], \qquad s_i = \sigma_i + \int [u_i - 2\,\mathrm{sign}(s_i)]\,\mathrm{d}\tau \tag{27}$$

B. Satellite Formation Control via Super-Twisting SOSM

The super-twisting SOSM controller (18) that provides a finite time convergence of the sliding variables and their derivatives to zero is designed for controlling the satellite formation model (22) and (23):

$$u_i = 3|\sigma_i|^{\frac{1}{2}}\,\mathrm{sign}(\sigma_i) + \int \mathrm{sign}(\sigma_i)\,\mathrm{d}\tau, \qquad \forall i = x, y, z \tag{28}$$

C. Satellite Formation Control via Continuous SMC Using ISSs

The continuous SMC with ISSs (20) and (21) is designed for controlling the satellite formation model (22) and (23):

$$\boldsymbol{u}_i = \frac{\tilde{\rho}_i}{2^{a_i}}\left|\boldsymbol{\sigma}_i + \tilde{k}_{0i}\int \mathrm{sign}(\boldsymbol{\sigma}_i)\,\mathrm{d}\tau\right|^{2a_i - 1} \mathrm{sign}\left[\boldsymbol{\sigma}_i + \tilde{k}_{0i}\int \mathrm{sign}(\sigma_i)\,\mathrm{d}\tau\right]$$

$$a_i = 0.9, \qquad \tilde{k}_{0i} = 0.5, \qquad \tilde{\rho}_i = 10, \qquad \forall i = x, y, z \tag{29}$$

Note that the control actions $\boldsymbol{u}_i$ in Eqs. (27–29) are continuous because the discontinuous high-frequency portions of the proposed control algorithm are filtered or integrated.

V. Simulations

A Simulink model of the follower satellite motion around the leader was developed to test the three continuous SMC methods' effectiveness against the same set of disturbances using Eqs. (22) and (23). For this study, the representative disturbance is a sine wave with amplitude of 0.5 km and a frequency of 0.6 rad/s (τ).

All three continuous SMC are compared with the traditional (discontinuous with dead band) SMC.[3] The same orbital period is used, that is, 100.7 min. Recall that τ is defined as the product of the mean motion and time. Therefore, for a 100.7-min orbit, the actual time required to reach $\tau = 1$ is 961.6 s. For the simulations, an Euler first-order integration algorithm is used, and the time step is held at a fixed 0.01 ms.

In Eq. (23), the values of parameters are taken as $r = 0.5$ km for the reference trajectory, whereas $r = 0.6$ km for the follower satellite to create the initial conditions offset. Also $n = 0.0$ and $m = \sqrt{3}$ are defined to put the follower satellite in a circular orbit around the leader at $\pm 2\pi/3$-rad inclination with the x axis. The angular position $\theta = -\pi/2$ is the same for both the reference trajectory and the simulated satellite's trajectory.

A PWM technique is used to turn the continuous SMC signals into a pulse train that could be realizable by a satellite jet thruster. It is assumed that the thruster can cycle at a frequency of 10 Hz. Because of the 961.6-s/τ conversion factor, 10-Hz signal in the time domain would need to be approximately 10,000 cycles/τ signal in the τ domain. Therefore, a dither signal, a sine wave of 10,000 cycles/τ with amplitude of 0.25×10^{-5} km/s^2, is combined with the control signal to model the duty cycle of the thrusters. To further optimize weekly fuel consumption, the dead zone is used in the relay elements of PWM. The recommended dead-band optimal value is taken[3] as $\delta_i = 0.5 \times 10^{-5}$ km/s^2 and the corresponding PWM with a dead band is shown in Fig. 2.

First, traditional (discontinuous with a dead band) SMC[3] was simulated and successfully reduced the initial position offset of the follower satellite after several hours. Then the follower was tracking the reference trajectory (23) fairly well. Simulations have verified

Table 1 Duty cycle analysis: SMC with dead zone

Simulation time step, ms	Approximate control input duty cycle, Hz	δ, km/s^2
0.1	2	0.5×10^{-5}
0.01	20	0.5×10^{-5}
0.001	200	0.5×10^{-5}

Table 2 Steady-state stabilization errors

	Method			
Tracking error, km	Traditional SMC	Continuous SMC driven by SMDO	Super-twisting control	Continuous SMC/ISS
$\lvert e_x\rvert$	3.6×10^{-4}	1.5×10^{-5}	2.2×10^{-5}	2.1×10^{-5}
$\lvert e_y\rvert$	3.4×10^{-4}	0.4×10^{-5}	0.5×10^{-5}	0.5×10^{-5}
$\lvert e_z\rvert$	3.7×10^{-4}	2.8×10^{-5}	4.2×10^{-5}	4.1×10^{-5}

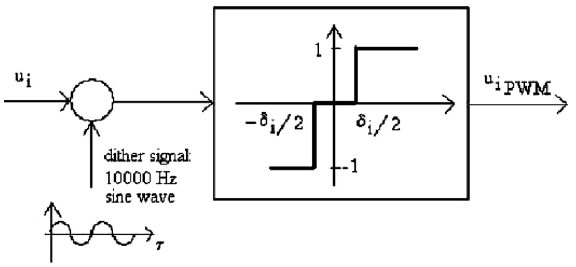

Fig. 2 PWM with dead band.

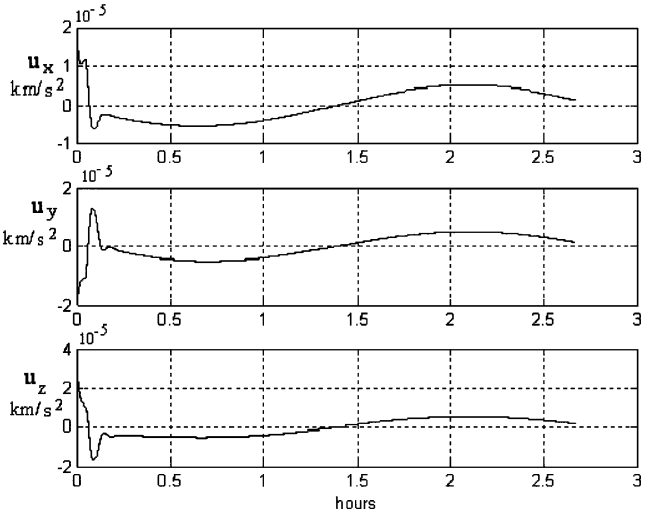

Fig. 3 Continuous SMC with SMDO.

that the frequency of switching is a function of the time step Δt of the simulation, whereas $\boldsymbol{\sigma}_i$ is at $\pm\delta_i/2$, and is not stabilized by a choice of δ_i. Table 1 shows how the Δt of the simulation effects the duty cycle of the controller. This deficiency of the traditional SMC with a dead band was successfully eliminated via use of proposed continuous SMC combined with PWM.

Figure 3 shows the control inputs to the follower satellite while using the continuous SMC driven by SMDO. After a few hours, this control drives the sliding variables and the errors to near zero. However, because this algorithm is supposed to be controlling a satellite thruster that fires pulses of thrust of constant magnitude, the continuous control input shown in Fig. 3 vs the original time t is not be very useful. Figure 4 shows the control inputs with the PWM technique implemented in the original time t. Here, the 10-Hz duty cycle is clearly shown. With the PWM technique, all continuous SMC reduce the errors between reference trajectory and the follower satellite's trajectory to near zero. The upper boundaries of steady-state errors are compared in Table 2.

Table 3 Weekly fuel consumption

Fuel consumption, m/s	Method			
	Traditional SMC	Continuous SMC driven by SMDO	Super-twisting control	Continuous SMC/ISS
ΔV_x	0.212	0.210	0.448	0.272
ΔV_y	0.203	0.202	0.428	0.252
ΔV_z	0.203	0.202	0.428	0.252

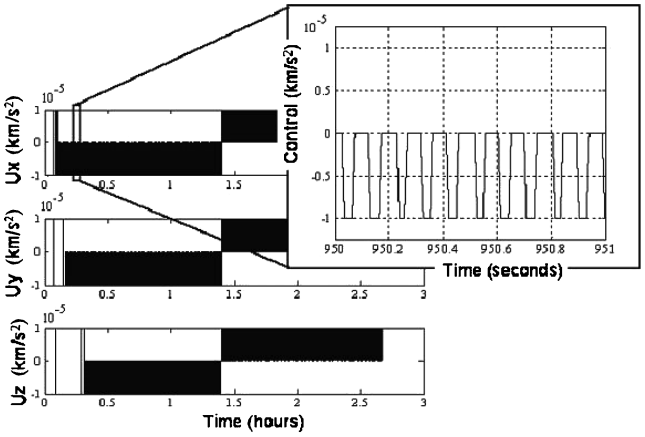

Fig. 4 Continuous SMC with SMDO modulated by PWM.

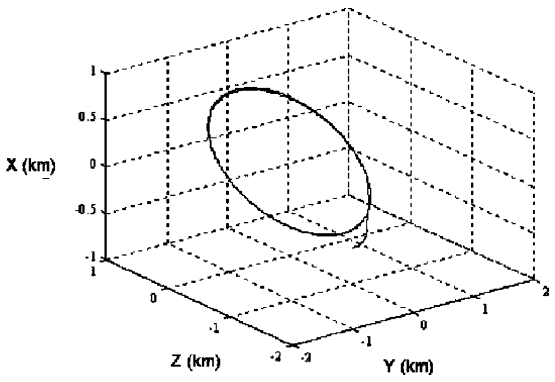

Fig. 5 Three-dimensional trajectory: continuous SMC with SMDO modulated by PWM.

Figure 5 shows the three-dimensional view of the relative motion between the leader and follower satellite using the continuous SMC driven by SMDO with the PWM technique incorporated. The other continuous SMC demonstrated similar performances. The corresponding weekly fuel consumptions in terms of ΔV, which are low for all methods, are shown in Table 3.

VI. Conclusions

Application of a variety of continuous SMC techniques, including SOSM, continuous SMC driven by SMDO, and continuous SMC using ISS, to satellite formation control are studied. The continuous robust to disturbances SMC laws easily drive the control thrusters with given duty cycle using the PWM technique, which is an improvement of a traditional (discontinuous with dead band) SMC. The simulation analysis shows that the continuous SMC/HOSM methods are effective in reducing the tracking errors of the follower satellite in the presence of a bounded disturbance function while keeping fuel consumption at a low level. It also appears that the PWM technique introduced does not degrade the tracking performance to any significant degree, retaining fixed duty cycle. Although the continuous SMC techniques were studied using a linearized satellite formation model, it is expected that studied the continuous SMC algorithms can easily handle the nonlinear uncertain models as well.

Appendix: Proof of the Theorem

First, we demonstrate that control (21) drives the auxiliary sliding variable η_i to a bounded domain $|\eta_i| \le \gamma_i$ via the Lyapunov function technique. Indeed, the dynamics of η_1 are derived as

$$\dot{\eta}_i = \psi_i^0(.) + \Delta\psi_i(.) + \tilde{k}_{0i}\,\mathrm{sign}(s_i) - \tilde{u}_i, \qquad k_{0i} > 0 \quad \text{(A1)}$$

A candidate for a Lyapunov function is introduced:

$$Q_i = \tfrac{1}{2}\eta_i^2 \quad \text{(A2)}$$

and its derivative is requested to satisfy the inequality

$$\dot{Q}_i \le -\rho_{0i} Q^{a_i}, \qquad 0.5 < a_i < 1.0 \quad \text{(A3)}$$

Meeting conditions (A2) and (A3) yields η_i, a finite time convergence to zero with

$$t_{ri} = [Q_i(0)]^{1-a_i} \big/ \rho_{0i}(1-a_i) \quad \text{(A4)}$$

Control function (21) being substituted in derivation (A1) yields inequality (A3) everywhere except for the domain

$$|\eta_i| \le \gamma_i = 2^{a_i}[(\tilde{L}_i + \tilde{k}_{0i})/(\tilde{\rho}_i - \rho_{0i})]^{1/(2a_i - 1)} \quad \text{(A5)}$$

Note that the domain of convergence (A5) can be designed arbitrary small by a corresponding selection of the gains ρ_{0i}, $\tilde{\rho}_i$, $\tilde{k}_{0i}$, and a_i. For instance, because $0 < 1/(2a_i - 1) < 1$ and $0 < \gamma_i < 1$, and given a_i, $\tilde{k}_{0i}$, and ρ_{0i}, then the value of the gain $\tilde{\rho}_i$ in Eq. (21) can be computed:

$$\tilde{\rho}_i > \rho_{0i} + 2^{a_i}(\tilde{L}_i + \tilde{k}_{0i}) \quad \text{(A6)}$$

Also, a corresponding bounded domain $D_i : \{\sigma_i, \dot{\sigma}_i\}$ that contains the origin can be identified such that if η_i satisfies inequality (A5), then $\boldsymbol{\sigma}_i, \dot{\boldsymbol{\sigma}}_i \in D_i$.

Second, a convergence of $\boldsymbol{\sigma}_i, \dot{\boldsymbol{\sigma}}_i \to 0$ is studied via a Lyapunov function analysis. The $\boldsymbol{\sigma}_i$ compensated dynamics are obtained:

$$\dot{\boldsymbol{\sigma}}_i = \psi_i^0(.) + \Delta\psi_i(.) - \left(\tilde{\rho}_i \big/ 2^{a_i}\right)|\eta_i|^{2a_i - 1}\,\mathrm{sign}(\eta_i)$$

$$\eta_i = \boldsymbol{\sigma}_i + \tilde{k}_{0i}\int \mathrm{sign}(\boldsymbol{\sigma}_i)\,\mathrm{d}\tau \quad \text{(A7)}$$

Differentiating Eq. (A7), we obtain for $a_i \to 1$,

$$\ddot{\sigma}_i + (\tilde{\rho}_i/2)\dot{\sigma}_i + k_{0i}(\tilde{\rho}_i/2)\,\mathrm{sign}(\sigma_i) = \Delta\dot{\psi}_i(.) \quad \text{(A8)}$$

which is rewritten as

$$\ddot{\sigma}_i + (\tilde{\rho}_i/2)\dot{\sigma}_i + [\tilde{k}_{0i}(\tilde{\rho}_i/2) - \Delta\dot{\psi}_i(.)\,\mathrm{sign}(\sigma_i)]\,\mathrm{sign}(\sigma_i) = 0 \quad \text{(A9)}$$

When $\tilde{\rho}_i$ in inequality (A6) is selected sufficiently large, the following inequality can be guaranteed:

$$[\tilde{k}_{0i}(\tilde{\rho}_i/2) - \Delta\dot{\psi}_i(.)\,\mathrm{sign}(\boldsymbol{\sigma}_i)]\,\mathrm{sign}(\boldsymbol{\sigma}_i)\,\boldsymbol{\sigma}_i > 0, \qquad \sigma_i \ne 0 \quad \text{(A10)}$$

This means that, given a sufficiently large $\tilde{\rho}_i$, it can be said that the mechanical work of this generalized force is always positive or

$$\int_0^{\sigma_i} [\tilde{k}_{0i}(\tilde{\rho}_i/2) - \Delta\psi_i(.)\,\mathrm{sign}(\xi)]\,\mathrm{sign}(\xi)\,\mathrm{d}\xi > 0 \quad \text{(A11)}$$

A candidate Lyapunov function is selected as

$$V_i = \left(\dot{\boldsymbol{\sigma}}_i^2 \big/ 2\right) + \int_0^{\sigma_i} [\tilde{k}_{0i}(\tilde{\rho}_i/2) - \Delta\dot{\psi}_i(.)\,\mathrm{sign}(\xi)]\,\mathrm{sign}(\xi)\,\mathrm{d}\xi > 0$$

$$\forall \boldsymbol{\sigma}_i \ne 0, \qquad \dot{\boldsymbol{\sigma}}_i \ne 0 \quad \text{(A12)}$$

and taking the derivative of this Lyapunov function yields

$$\begin{aligned}\dot{V}_i &= \dot{\boldsymbol{\sigma}}_i\ddot{\boldsymbol{\sigma}}_i + \tilde{k}_{0i}(\tilde{\rho}_i/2)\,\mathrm{sign}(\boldsymbol{\sigma}_i)\dot{\boldsymbol{\sigma}}_i - \Delta\ddot{\psi}_i(.)\boldsymbol{\sigma}_i - \Delta\dot{\psi}_i(.)\dot{\boldsymbol{\sigma}}_i \\ &= -(\tilde{\rho}_1/2)\dot{\boldsymbol{\sigma}}_i^2 - \Delta\ddot{\psi}_i(.)\boldsymbol{\sigma}_i \le -(\tilde{\rho}_i/2)\dot{\boldsymbol{\sigma}}_i^2 + \tilde{L}_i|\boldsymbol{\sigma}_i| \\ &= \tilde{L}_i|\boldsymbol{\sigma}_i|\left[1 - (\tilde{\rho}_i/2)\left(\dot{\boldsymbol{\sigma}}_i^2\Big/\tilde{L}_i|\boldsymbol{\sigma}_i|\right)\right] < 0 \end{aligned} \tag{A13}$$

This leads to the selection of $\tilde{\rho}_i$ as

$$\tilde{\rho}_i > 2\left(\dot{\boldsymbol{\sigma}}_i^2\Big/\tilde{L}_i|\boldsymbol{\sigma}_i|\right) \ge (2/\tilde{L}_i)M \tag{A14}$$

Thus, there exists some $\tilde{\rho}_i$ such that $V_i > 0$ and $\dot{V}_i < 0$, which proves the local asymptotic stability of the origin $\boldsymbol{\sigma}_i = \dot{\boldsymbol{\sigma}}_i = 0$, and that the sliding variable σ_i converges asymptotically into a second-order sliding mode, $\dot{\boldsymbol{\sigma}}_i = \boldsymbol{\sigma}_i = 0$.

References

[1]Yeh, H., and Sparks, A., "Geometry and Control of Satellite Formations," *Proceedings of the American Control Conference*, IEEE Publications, Piscataway, NJ, 2000, pp. 384–388.

[2]Sparks, A., "Satellite Formation Keeping Control in the Presence of Gravity Perturbations," *Proceedings of the American Control Conference*, IEEE Publications, Piscataway, NJ, 2000, pp. 844–848.

[3]Yeh, H., Nelson, E., and Sparks, A., "Nonlinear Tracking Control for Satellite Formations," *Journal of Guidance, Control, and Dynamics*, Vol. 25, No. 2, 2002, pp. 376–386.

[4]Utkin, V., Guldner, J., and Shi, J., *Sliding Modes in Electromechanical Systems*, Taylor and Francis, London, 1999, pp. 147–153.

[5]Levant, A., "Universal Single-Input-Single-Output (SISO) Sliding-Mode Controllers with Finite-Time Convergence," *IEEE Transactions on Automatic Control*, Vol. 46, No. 9, 2001, pp. 1447–1451.

[6]Brown, M., and Shtessel, Y. B., "Disturbance Rejection Techniques for Finite Reaching Time Continuous Sliding Mode Control," *Proceedings of the American Control Conference*, Vol. 6, IEEE Publications, Piscataway, NJ, 2001, pp. 4998–5003.

[7]Massey, T., and Shtessel, Y., "Satellite Formation Control Using Traditional and High Order Sliding Modes," AIAA Paper 2004-5021, Aug. 2004.

[8]Isidori, A., *Nonlinear Control Systems*, 3rd ed., Springer-Verlag, London, 1995.

[9]Poularikas, A. D., and Seely, S., *Signals and Systems*, Krieger, Malabar, FL, 1994.